Virologica Sinica 40 (2025) 921–934

Contents lists available at ScienceDirect

Virologica Sinica

journal homepage: www.keaipublishing.com/en/journals/virologica-sinica
www.virosin.org

Research article

RNA and ChIP-sequencing analysis reveals SOX3 suppresses antiviral innate immunity through the AKT1-PTEN signaling axis

Tanzeel Yousaf [a], Jianwen Chen [a], Wajeeha Naz [a], Jiaqi Xu [a], Ying Liu [b], Junsong Huang [b], Siqi Yang [a], Jing Zhang [a], Iram Amin [c], Mingxiong Guo [b], Yunlan Tang [d,*], Guihong Sun [a,e,*]

[a] Taikang Medical School (School of Basic Medical Sciences), Wuhan University, Wuhan 430071, China
[b] Hubei Key Laboratory of Cell Homeostasis, College of Life Sciences, Wuhan University, Wuhan 430072, China
[c] Centre of Excellence in Molecular Biology (CEMB), University of the Punjab, Lahore 53700, Pakistan
[d] Henan Provincial People's Hospital, Henan Eye Hospital, Henan Eye Institute, People's Hospital of Zhengzhou University, Henan University People's Hospital, Zhengzhou 450003, China
[e] Hubei Provincial Key Laboratory of Allergy and Immunology, Wuhan 430071, China

ARTICLE INFO

Keywords:
Sex-determining region Y-box protein 3 (SOX3)
Type I interferons (IFN-I)
Interferon-stimulated genes (ISGs)
Antiviral innate immunity
AKT serine/threonine kinase 1 (AKT1)

ABSTRACT

The transcription factor Sex-determining region Y-box protein 3 (SOX3) is well known for its critical roles in sex determination and cell differentiation; however, its function in antiviral innate immunity remains unexplored. This study uncovered how SOX3, induced by viral infections, modulates type I interferon (IFN–I) responses. RNA sequencing, quantitative PCR, and immunoblot analysis collectively revealed that SOX3 overexpression suppresses virus-induced interferon beta 1(IFN-β) promoter activation and significantly inhibits the expression of key antiviral interferon-stimulated genes (ISGs), including ISG15 and interferon induced protein with tetratricopeptide repeats 1 (IFIT1). Conversely, the knockdown of SOX3 enhanced IFN-β production and ISGs expression, confirming its role as a negative regulator of antiviral immunity. Mechanistically, chromatin immunoprecipitation sequencing (ChIP-seq) identified SOX3 binding specifically at the AKT serine/threonine kinase 1 (AKT1) locus. Further analysis demonstrated that SOX3 directly upregulates AKT1 expression, subsequently increasing phosphorylation and inactivation of the tumor suppressor phosphatase and tensin homolog (PTEN). Inactivation of PTEN inhibited interferon regulatory factor 3 (IRF3) nuclear translocation, leading to reduced IFN-β expression. Thus, our findings uncover a previously uncharacterized SOX3-AKT1-PTEN signaling axis in the regulation of antiviral innate immunity, providing new insights into immune evasion strategies and highlighting potential therapeutic targets to enhance antiviral responses.

INTRODUCTION

The innate immune system provides the first line of defense against invading pathogens, with IFNs-I playing a pivotal role in controlling viral infections (Cao et al., 2018; Fensterl and Sen, 2009; Sun et al., 2020). Upon viral invasion, germline-encoded pattern recognition receptors (PRRs) such as RIG-I-like receptors (RLRs), Toll-like receptors (TLRs), and NOD-like receptors (NLRs) recognize viral pathogen-associated molecular patterns (PAMPs), including viral nucleic acids and proteins. This recognition triggers the production of type-I IFNs, primarily IFN-β, which orchestrates a potent antiviral response (Cao et al., 2018; Jang et al., 2015; Kasuga et al., 2021; Takeuchi and Akira, 2009). IFN-β then initiates a cascade of signaling events, leading to the expression of interferon-stimulated genes (ISGs) and establishing an antiviral state. While the core components of the type I IFN pathway are well-characterized, many regulatory mechanisms remain to be elucidated.

SOX3, a member of the SOX (Sry-related HMG box) family of transcription factors (TFs), is crucial for sex determination and cell differentiation (Del Puerto et al., 2024; Jiang et al., 2024). SOX4, induced

* Corresponding authors.
E-mail addresses: 16110700022@fudan.edu.cn (Y. Tang), ghsunlab@whu.edu.cn (G. Sun).

https://doi.org/10.1016/j.virs.2025.11.012
Received 17 April 2025; Accepted 27 November 2025
Available online 5 December 2025

during viral infections, suppresses the TLR signaling pathway by inhibiting key components such as MyD88, IRAK4, and TRIF, while attenuating NF-κB and IRF3/7 activation (Shang et al., 2021). Similarly, SOX2 has been implicated in innate immunity, acting as a neutrophil DNA sensor to combat microbial infections (Xia et al., 2015). Interestingly, our group recently revealed that SOX3 promotes hepatocarcinogenesis via the AKT1-mTOR signalling pathway (Liu et al., 2025). However, the role of SOX3 in antiviral immunity remains unexplored. AKT1, a serine/threonine-protein kinase initially identified as a retroviral oncogene, can modulate the development and function of innate immune cells, including neutrophils, macrophages, and dendritic cells (Zhang et al., 2013). Activated AKT1 phosphorylates numerous substrates, promoting various cellular processes such as cell survival, growth, migration, angiogenesis, protein synthesis, and glucose metabolism (Wan et al., 2021). One such key substrate is the PTEN, a well-established tumour suppressor that also functions as a negative regulator of AKT signalling (Lee et al., 2018; Steinbach et al., 2019; Zhang et al., 2023). PTEN has also been shown to play a critical role in antiviral innate immunity by dephosphorylating IRF3, a crucial transcription factor for IFN-β production (Li et al., 2016; Taylor et al., 2019). The molecular mechanism by which the SOX3-AKT1-PTEN pathway contributes to antiviral innate immunity is not yet elucidated. Therefore, further research is necessary to understand the upstream regulatory factors that control type I interferon activity.

In this study, we identified a novel role of the transcription factor SOX3 in antiviral innate immunity. We demonstrated that SOX3 induced by viral infections modulates IFNs-I responses. Combined results from RNA sequencing (RNA-seq), quantitative PCR, and immunoblot analysis revealed that SOX3 overexpression suppresses virus-induced IFN-β promoter activation and significantly inhibits the expression of key antiviral ISGs, including ISG15 and IFIT1. In contrast, the downregulation of endogenous SOX3 promotes IFN-β expression. Chromatin immunoprecipitation (ChIP)-seq analysis revealed that SOX3 directly binds to the AKT1 promoter, leading to upregulation of AKT1 expression. This leads to increased PTEN phosphorylation, its subsequent inactivation, impaired nuclear translocation of IRF3, and consequently, diminished type I interferon expression. Our findings uncover a previously uncharacterized regulatory role of the SOX3 involving the AKT1-PTEN pathway, providing novel insights into viral immune evasion mechanisms and offering a potential therapeutic target to enhance antiviral innate immunity.

RESULTS

Genome-wide transcriptional modulation by SOX3 in SeV-infected HEK293T cells

Previously, SOX2 and SOX4 were reported to be involved in innate immunity (Shang et al., 2021; Xia et al., 2015). Based on this, we hypothesized that another member of the SOX family, SOX3, might also contribute to antiviral innate immunity, a role that has not yet been explored. To test this hypothesis, we examined how SOX3 influences IFN-I activation in response to viral infection.

We first evaluated the transcriptional profiles of HEK293T cells infected with or without Sendai virus (SeV) and with or without SOX3 overexpression (SOX3SeV, VECSeV, SOX3, VEC) by identifying differentially expressed genes (P-value ≤ 0.05, fold change >1.0). Volcano plots were employed to visualize gene expression variation, revealing that the number of genes with significantly altered expression varied across different conditions (control or SOX3 expression, with or without SeV infection). The highest number of altered genes observed in SOX3SeV vs mock (VECSeV, SOX3, and VEC) with 4034 genes which were primarily involved in the type I interferon response (*IFNB1, IFNE, IFNL1, IFIT1, IFIT2, IFIH1*), antiviral response (*ISG15, ISG20, OASL*), and proinflammatory cytokines and chemokines (*TNFSF13B, CCL2, CCL8, CXCL8, CXCL1, CXCL10, CXCL11*) (Fig. 1A, Supplementary Fig. S1A and B). To identify signaling pathways affected by SOX3 in SeV-infected HEK293T cells, we performed gene ontology and pathway analysis (Fig. 1B, Supplementary Fig. S1C). SOX3SeV vs mock cells showed diminished induction of genes involved in the antiviral innate immune response (Fig. 1C and D, Supplementary Fig. S2A), proinflammatory cytokine signalling (Fig. 1E and F, Supplementary Fig. S2B), the pattern recognition receptor (PRR) response (Supplementary Fig. S3A and B), and antigen presentation (Supplementary Fig. S3C and D). Overall, these results indicate that SOX3 overexpression in SeV-infected HEK293T cells leads to the downregulation of key immune response genes, including those involved in type I interferon signaling, antiviral defense, and proinflammatory cytokine production, highlighting its role in modulating the immune response during viral infection.

SOX3 suppresses virus-induced type I interferon activation

To validate our transcriptomic findings, we overexpressed SOX3 in HEK293T and A549 cells and performed a pGL3-IFN-β promoter luciferase reporter assay, which revealed that SOX3 significantly inhibited SeV and herpes simplex virus type 1 (HSV-1)-induced IFN-β promoter activation in a dose-dependent manner (Fig. 2A; Supplementary Fig. S4A). We then assessed the impact of SOX3 overexpression on SeV and HSV-1-induced IFN-β mRNA expression. Quantitative real-time PCR analysis revealed that SOX3 overexpression significantly reduced virus-induced IFNB1 expression in a dose-dependent manner (Fig. 2B; Supplementary Fig. S4B). Since IFN-β activation leads to the expression of downstream ISGs (Kishimoto et al., 2021; Lang et al., 2022; Schneider et al., 2014), we next evaluated the effects of SOX3 on ISGs expression. SOX3 overexpression markedly inhibited the expression of ISG15 (Fig. 2C; Supplementary Fig. S4C, left panel) and IFIT1 (Fig. 2C; Supplementary Fig. S4C, right panel), which are key ISGs involved in the antiviral response (Diamond and Farzan, 2013; McDougal et al., 2024; Perng and Lenschow, 2018; Zhang et al., 2021).

IFN-I expression occurs in two phases: an initial rapid phase, where pattern recognition receptors (PRRs) detect viral pathogen-associated molecular patterns (PAMPs), activating IRF3 to induce IFN-β production, and a second phase of positive feedback involving IRF7(Li et al., 2016; Ning et al., 2011; Popli et al., 2022). To investigate the role of SOX3 in these stages, we measured IFNB1 and ISG15 mRNA levels at various time intervals following SeV infection. SOX3 overexpression suppressed both IFNB1 and ISG15 mRNA expression from 6 to 15 h post-infection (Fig. 2D, left and right panels), suggesting that SOX3 inhibits the antiviral response at both the early and late stages of IFN production. These findings indicate that SOX3 effectively dampens virus-induced IFN-β activation, highlighting its role in modulating antiviral immune responses.

Induction of SOX3 during viral infection inhibits key antiviral innate immune pathways

The involvement of SOX3 in antiviral responses was further explored by analyzing its expression during viral infection. Immunoblot analysis revealed a significant upregulation of SOX3 protein expression in HEK293T cells following SeV infection (Fig. 3A). To explore the broad antiviral innate immunity role of SOX3, we investigated its induction in response to different viral infections. This induction of SOX3 was also observed at the mRNA level in THP-1 cells infected with SeV, vesicular stomatitis virus (VSV), or HSV-1 (Fig. 3B). These findings indicate that SOX3 expression is induced by diverse viral infections, suggesting a potential role in modulating antiviral immune responses against both RNA and DNA viruses.

Next, we investigated the impact of SOX3 on key antiviral signaling pathways; overexpression of SOX3 significantly suppressed IFN-β promoter activation induced by RIG-I, TBK1, and MAVS in HEK293T cells (Fig. 3C–E). This inhibitory effect suggests that SOX3 negatively regulates antiviral signaling by suppressing these key upstream components

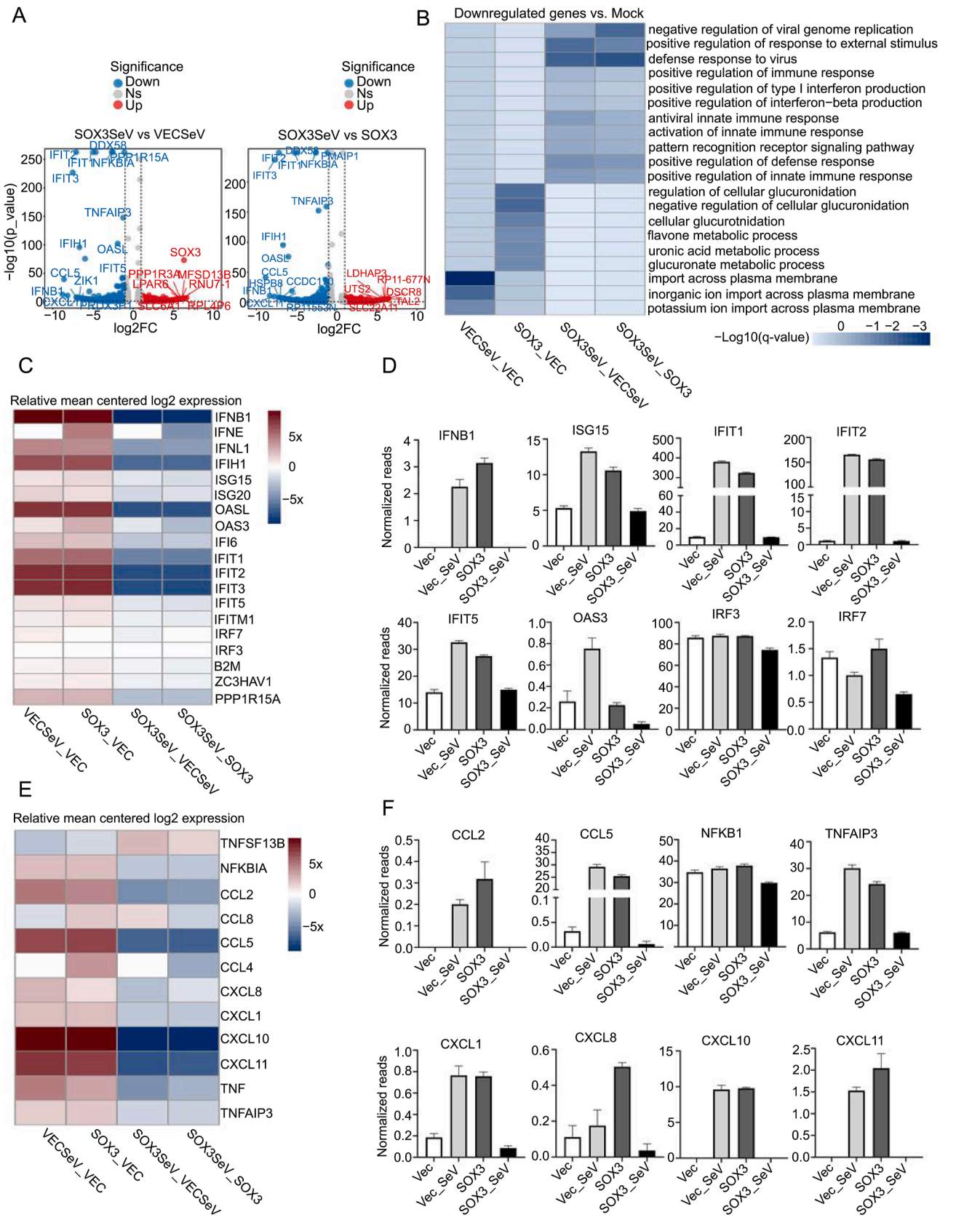

(caption on next page)

of the IFN-β pathway. We further explored the role of SOX3 in IFN-I responses by assessing IFN-β promoter activity in RAW264.7 macrophages stimulated with various ligands, including PBS, lipopolysaccharide (LPS), and synthetic RNA duplex poly (I:C). SOX3 overexpression significantly suppressed IFN-β activation in response to all these stimuli (Fig. 3F), indicating that SOX3 negatively regulates IFN-β production in a manner independent of the specific stimulus and cell type.

Finally, we assessed the impact of SOX3 on broader antiviral signaling, including interferon-stimulated response element (ISRE) and nuclear factor kappa-light-chain-enhancer of activated B cells (NF-κB). SOX3 overexpression inhibited SeV-induced ISRE promoter activity (Fig. 3G) and reduced SeV-induced NF-κB activation in a dose-dependent manner (Fig. 3H). Taken together, these results demonstrate that SOX3 is induced during viral infection and functions as a negative regulator of antiviral innate immunity by broadly suppressing signaling pathways, including those mediated by RIG-I, TBK1, MAVS, ISRE, and NF-κB.

SOX3 knockdown enhances antiviral responses

We then explored whether SOX3 knockdown could enhance antiviral immune responses by examining its effects on IFN-β activation and the expression of key ISGs. To confirm the specificity of SOX3 knockdown and rule out potential off-target effects, we used both siRNA and sgRNA. We first confirmed efficient knockdown of SOX3 in HEK293T cells transfected with either SOX3-targeting siRNAs (si*SOX3*) and sgRNAs (sgSOX3) compared to cells transfected with non-targeting controls, as demonstrated by immunoblot analysis (Fig. 4A). Subsequently, SeV-induced IFN-β promoter activity was significantly suppressed by Flag-SOX3 overexpression, and this inhibitory effect was relieved by co-expression of Lenti-V2-sgSOX3, validating the specificity of SOX3's negative regulatory role. (Fig. 4B). This increase in IFN-β promoter activity was accompanied by a significant elevation in IFNB1 mRNA expression following SeV and HSV-1 infection, as determined by quantitative RT-PCR (Fig. 4C; Supplementary Fig. S5A). These results indicate that SOX3 negatively regulates IFN-β expression during antiviral responses.

To further examine the downstream effects of SOX3 knockdown, we assessed the expression levels of the ISGs (ISG15 and IFIT1). SOX3 depletion significantly increased the expression of both ISG15 and IFIT1 following SeV and HSV-1 infection (Fig. 4D; Supplementary Fig. S5B. These results demonstrate that the absence of SOX3 enhances antiviral immune responses, further supporting its role as a negative regulator of IFN-I and antiviral signaling pathways.

ChIP-seq analysis unveils SOX3 binding repertoire in HSV-1 infection

While our study initially examined the antiviral response to SeV infection, we expanded our investigation to include HSV-1 for the ChIP-seq analysis in order to explore the broader generalizability of SOX3 as a negative regulator of immune responses. By incorporating both RNA (SeV) and DNA (HSV-1) viruses, we aimed to evaluate the versatility of SOX3 in regulating antiviral responses across different viral types. This approach provides insights into whether SOX3 functions as a negative regulator of type I IFN and ISG expression, contributing to immune evasion strategies across a broader spectrum of viral infections.

To investigate how SOX3 modulates antiviral responses, we performed ChIP-seq analysis to identify SOX3 binding sites in HEK293T cells with and without virus stimulation. Flag-tagged SOX3 was immunoprecipitated using a Flag antibody, and the resulting DNA fragments were sequenced and analyzed to assess changes in SOX3 binding following HSV-1 infection. Analysis of the distribution of SOX3 ChIP-seq reads in HEK293T cells showed specific enrichment in intergenic and intronic regions, confirming the reliability of the ChIP-seq analysis and efficient capture of SOX3-bound chromatin (Supplementary Fig. S6A and B). The average read counts for SOX3 binding relative to the transcription start site (TSS) revealed differential binding patterns between HSV-1 infected and mock-infected cells, with significant shifts in SOX3 binding following viral infection (Fig. 5A and Supplementary Fig. S6C). In particular, a pronounced enrichment of SOX3 binding is observed in HSV-1 infected cells compared to the mock conditions, with peaks near the TSS region suggesting a potential role for SOX3 in regulating genes during HSV-1 infection (Fig. 5B). A substantial number of binding sites (1051) were unique to the HSV-1 infected condition, indicating that viral infection induces specific recruitment of SOX3 to chromatin (Fig. 5C, top panel). The number of SOX3-bound peaks increased significantly in HSV-1-infected cells (1221 peaks) compared to mock controls (456 peaks), reflecting the role of SOX3 as a virus-induced regulator of transcriptional changes (Fig. 5C, bottom panel, Supplementary Fig. S6D; Supplementary Tables S1 and S2). We then investigated the impact of SOX3 differentially bound gene expression. A significant number of upregulated genes (546) were associated with SOX3 binding, including 427 genes with fold changes ≥2 (Fig. 5D and Supplementary Fig. S7A–C).

To explore the potential biological functions of SOX3 during HSV-1 infection, we performed Gene Ontology (GO) analysis of SOX3-differentially bound genes. This analysis revealed an upregulation of molecular functions involving protein kinases (AKT1, CASR, ESR1, and ROR2) and phosphatidylinositol binding, potentially modulating to the inflammatory and interferon response pathways (Hendy and Canaff, 2016; Hsu et al., 2010; Liu and Cohen, 2015; Yang et al., 2020) (Fig. 5E, top panel; Supplementary Table S3). In contrast, SOX3 downregulated molecular functions such as metal ion transport, neurotransmitter receptor activity, and SNARE binding, which could impair cytokine release and immune cell activation and disrupt calcium signaling and cAMP regulation (de Jesus and de Araújo Andrade, 2020; Stow et al., 2006; Tavares et al., 2020; Vig and Kinet, 2009) (Fig. 5E, bottom panel; Supplementary Table S4). This inhibition of key cellular processes could contribute to immune evasion and reduced antiviral immunity. Altogether, ChIP-seq analysis reveals that SOX3 binding is significantly altered during HSV-1 infection, likely impacting the expression of immune-related genes.

Fig. 1. Genome-wide transcriptional modulation by SOX3 in SeV-infected HEK293T cells. The cells were transfected for 24 h with plasmids encoding Flag-SOX3 and pEF-Flag and were then stimulated or left unstimulated with SeV at an MOI of 10 for 8 h. **A** Volcano plots are shown as -log10 adjusted *P* value (adjPval) versus log2 Fold change (FC). Differentially expressed genes in SOX3SeV versus VECSeV (left panel) and SOX3SeV versus SOX3 (right panel) conditions with an adjusted *P* value < 0.05 and fold change >1 is shown as colored dots. The names of the most significant genes are indicated in the plots. **B** Heatmaps of the top enriched functional annotations of genes significantly downregulated (adjusted *P* value < 0.05) across the comparisons of VECSeV vs VEC, SOX3 vs VEC, SOX3SeV vs VECSeV, and SOX3SeV vs SOX3. **C** Heatmap depicting relative transcription of type I interferon genes and ISGs for the comparisons between VECSeV vs VEC, SOX3 vs VEC, SOX3SeV vs VECSeV, and SOX3SeV vs SOX3. The data are the average of three experiments. **D** Gene expression values of type I interferon genes and ISGs from RNAseq in VEC, VECSeV, SOX3, and SOX3 SeV. Data are the mean (±SEM) of three experiments. **E** Heatmap of the relative expression of selected genes involved in proinflammatory signaling under the conditions of VECSeV vs VEC, SOX3 vs VEC, SOX3SeV vs VECSeV, and SOX3SeV vs SOX3. The data are the average of three experiments. **F** Gene expression values of proinflammatory signaling from RNAseq in VEC, VECSeV, SOX3, and SOX3SeV. Data are the mean (±SEM) of three experiments.

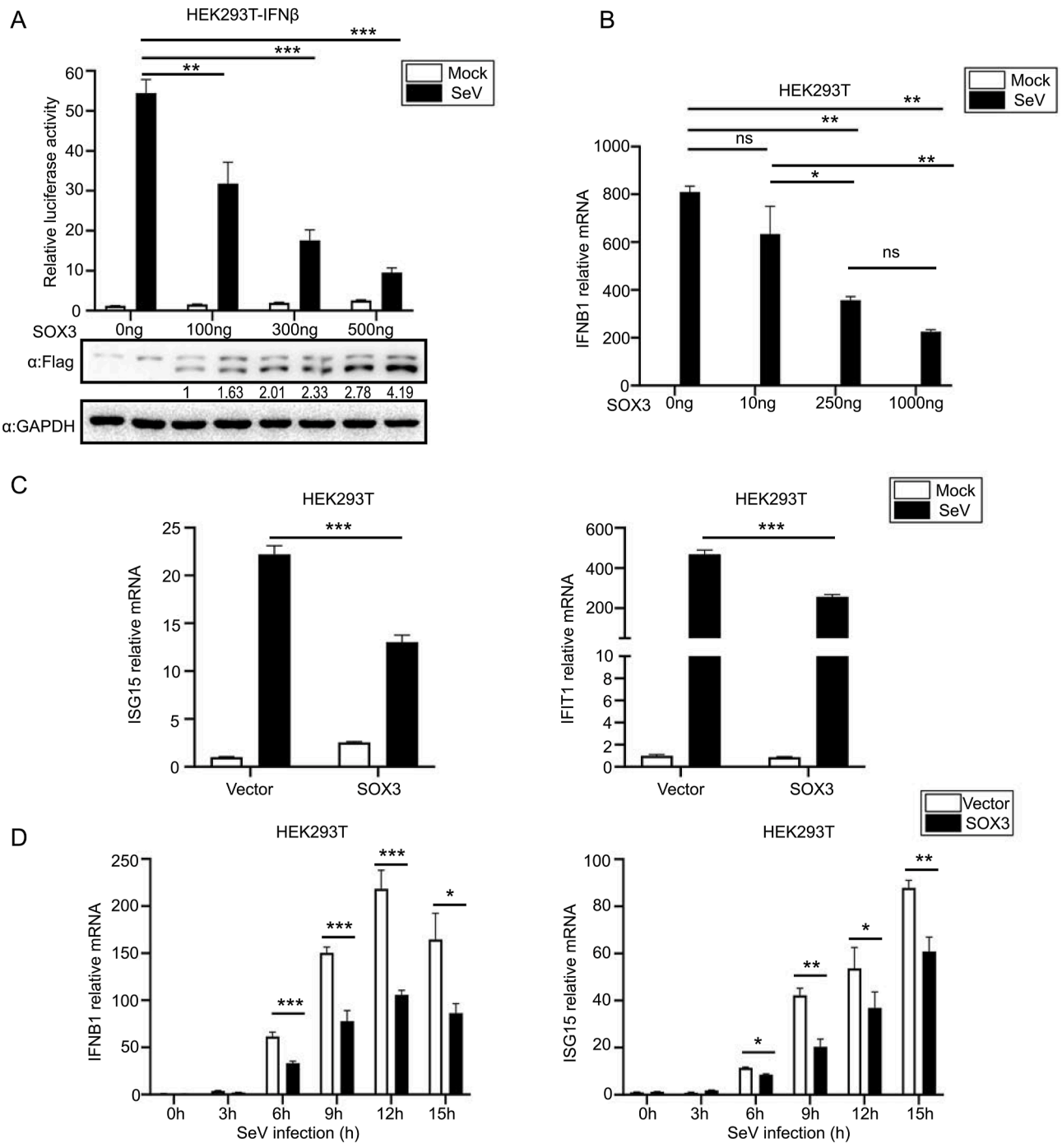

Fig. 2. SOX3 inhibits virus-induced activation of IFN-β. **A** Luciferase assay analyzing *IFNB1* promoter activity (top) and immunoblot analysis of Flag-SOX3 and GAPDH (loading control) (below) in HEK293T cells transfected for 24 h with a plasmid encoding an IFN-β firefly luciferase reporter (IFN-β–Luc), along with pEF-Flag, pRL-TK, or increasing doses of pEF-Flag-SOX3 plasmids, and cells were left stimulated or unstimulated with SeV at an MOI of 10 for 8 h; luciferase reporter activity is normalized to that of renilla luciferase. **B** Quantitative RT-PCR analysis of *IFNB1* mRNA in HEK293T cells transfected with pEF-Flag or increasing doses of pEF-Flag-SOX3 plasmids. After 24 h, cells were left stimulated or unstimulated for 8 h with SeV (MOI = 10). **C** Quantitative RT-PCR analysis of *ISG15* (left panel) and *IFIT1* (right panel) mRNA in HEK293 cells transfected with pEF-Flag or pEF-Flag-SOX3 plasmids. After 24 h, cells were left stimulated or unstimulated for 8 h with SeV (MOI = 10). **D** Quantitative RT-PCR analysis of *IFNB1* (left panel) and *ISG15* (right panel) mRNA in HEK293T cells transfected with pEF-Flag or pEF-Flag-SOX3 plasmids. After 24 h, cells were infected for 0–15 h (horizontal axis) with SeV (MOI = 10). The *P*-values in (**A**–**D**) were calculated using Student's *t*-test. Data are presented as mean ± SEM, with statistical significance indicated (***$P < 0.001$, **$P < 0.01$, *$P < 0.05$).

AKT1 is a key gene upregulated by SOX3 during viral infection

Building on the ChIP-seq analysis, we examined the expression of genes with differential SOX3 binding in SOX3-overexpressing HEK293T cells infected with or without HSV-1, aiming to identify key regulators of the antiviral response. This analysis revealed a significant increase in SOX3 binding at the AKT1, MAVS, and PTEN loci in HSV-1-infected cells overexpressing Flag-SOX3, compared to control conditions (Fig. 6A; Supplementary Fig. S8A and B). Among these genes, AKT1 emerged as a prominent candidate, showing pronounced SOX3 enrichment at its promoter region specifically in HSV-1-infected cells, supporting the notion that SOX3 may directly regulate AKT1 expression during viral

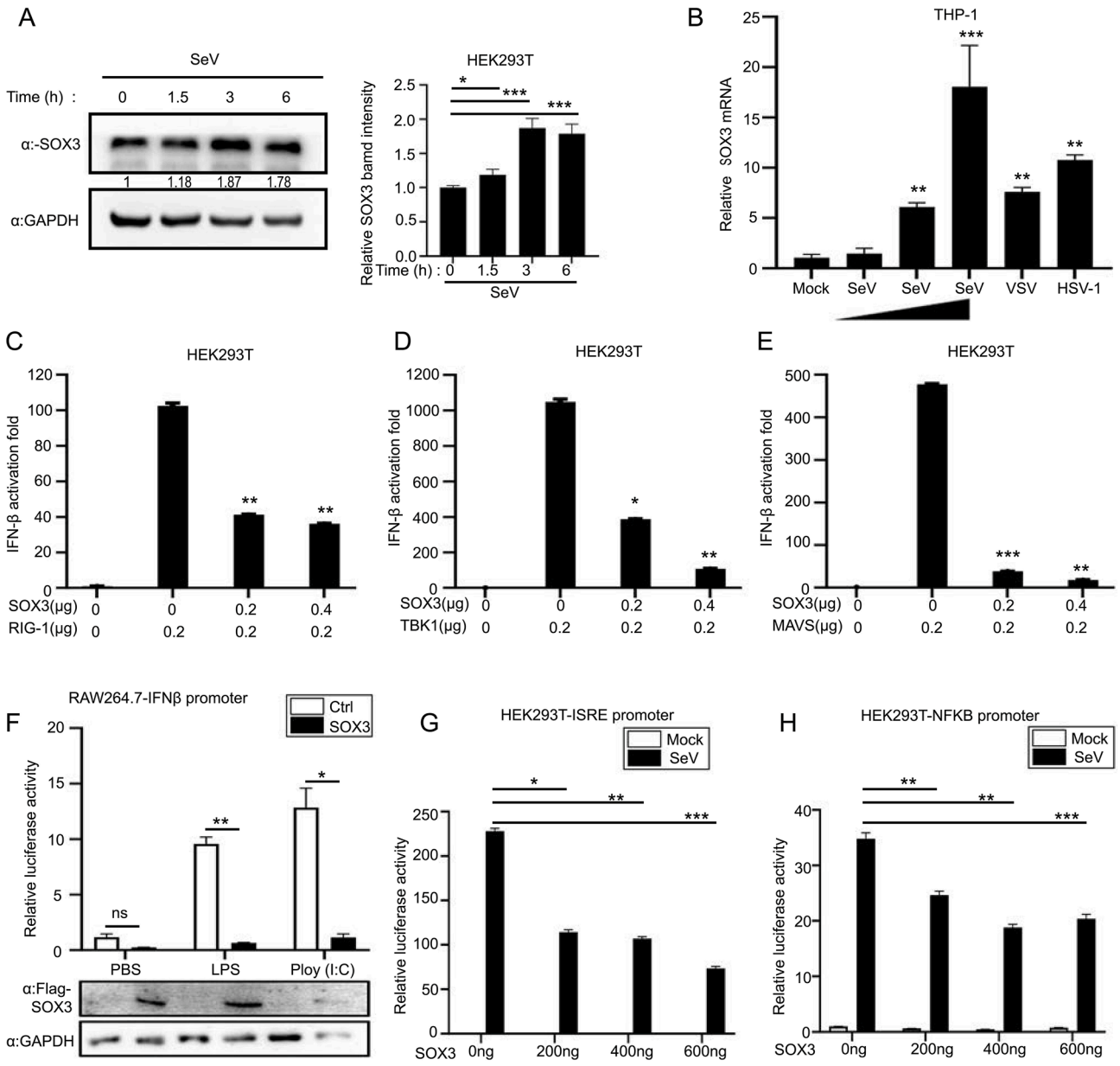

Fig. 3. SOX3 modulates antiviral immune signaling pathways in response to diverse stimuli. **A** Immunoblot analysis of SOX3 and GAPDH (loading control) in HEK293T cells, and cells were left stimulated with SeV at an MOI of 10 for 8 h (left panel). Quantification of SOX3 band intensity normalized to GAPDH (right panel). **B** Quantitative RT-PCR analysis of *SOX3* mRNA in THP-1 cells, after 36 h, cells were left infected for another 12 h with SeV, Vesicular Stomatitis Virus (VSV) (MOI = 0.1), and HSV-1 (MOI = 10). **C** Luciferase assay analyzing *IFNB1* promoter activity in HEK293T cells transfected for 48 h with a plasmid encoding an IFN-β firefly luciferase reporter (IFN-β–Luc), along with pEF-Flag, pEF-RIG-1, pRL-TK, or increasing doses of pEF-Flag-SOX3 plasmids; luciferase reporter activity is normalized to that of renilla luciferase. **D** Luciferase assay analyzing *IFNB1* promoter activity in HEK293T cells transfected for 48 h with a plasmid encoding an IFN-β firefly luciferase reporter (IFN-β-Luc), along with pEF-Flag, pEF-TBK1, pRL-TK, or increasing doses of pEF-Flag-SOX3 plasmids; luciferase reporter activity is normalized to that of renilla luciferase. **E** Luciferase assay analyzing *IFNB1* promoter activity in HEK293T cells transfected for 48 h with a plasmid encoding an IFN-β firefly luciferase reporter (IFN-β-Luc), along with pEF-Flag, pEF-MAVS, pRL-TK, or increasing doses of pEF-Flag-SOX3 plasmids; luciferase reporter activity is normalized to that of renilla luciferase. **F** Luciferase assay analyzing *IFNB1* promoter activity in RAW264.7 cells transfected for 24 h with a plasmid encoding an IFN-β firefly luciferase reporter (IFN-β-Luc), along with pEF-Flag, pRL-TK, or pEF-Flag-SOX3 plasmids, and were stimulated for 10 h with PBS, bacterial lipopolysaccharide (LPS), and poly (I:C); luciferase reporter activity is normalized to that of renilla luciferase. **G** Luciferase assay analyzing ISRE promoter activity in HEK293T cells transfected for 24 h with a plasmid encoding an ISRE firefly luciferase reporter (ISRE–Luc), along with pEF-Flag, pRL-TK, or increasing doses of pEF-Flag-SOX3 plasmids, and cells were left stimulated or unstimulated with SeV for 8 h; luciferase reporter activity is normalized to that of renilla luciferase. **H** Luciferase assay analyzing NFκB promoter activity in HEK293T cells transfected for 24 h with a plasmid encoding an ISRE firefly luciferase reporter (NFκB-Luc), along pEF-Flag, pRL-TK, or increasing doses of pEF-Flag-SOX3 plasmids, and cells were left stimulated or unstimulated with SeV for 8 h; luciferase reporter activity is normalized to that of renilla luciferase. The *P*-values in (**A**–**H**) were calculated using Student's *t*-test. Data are presented as mean ± SEM, with statistical significance indicated (***$P < 0.001$, **$P < 0.01$, *$P < 0.05$).

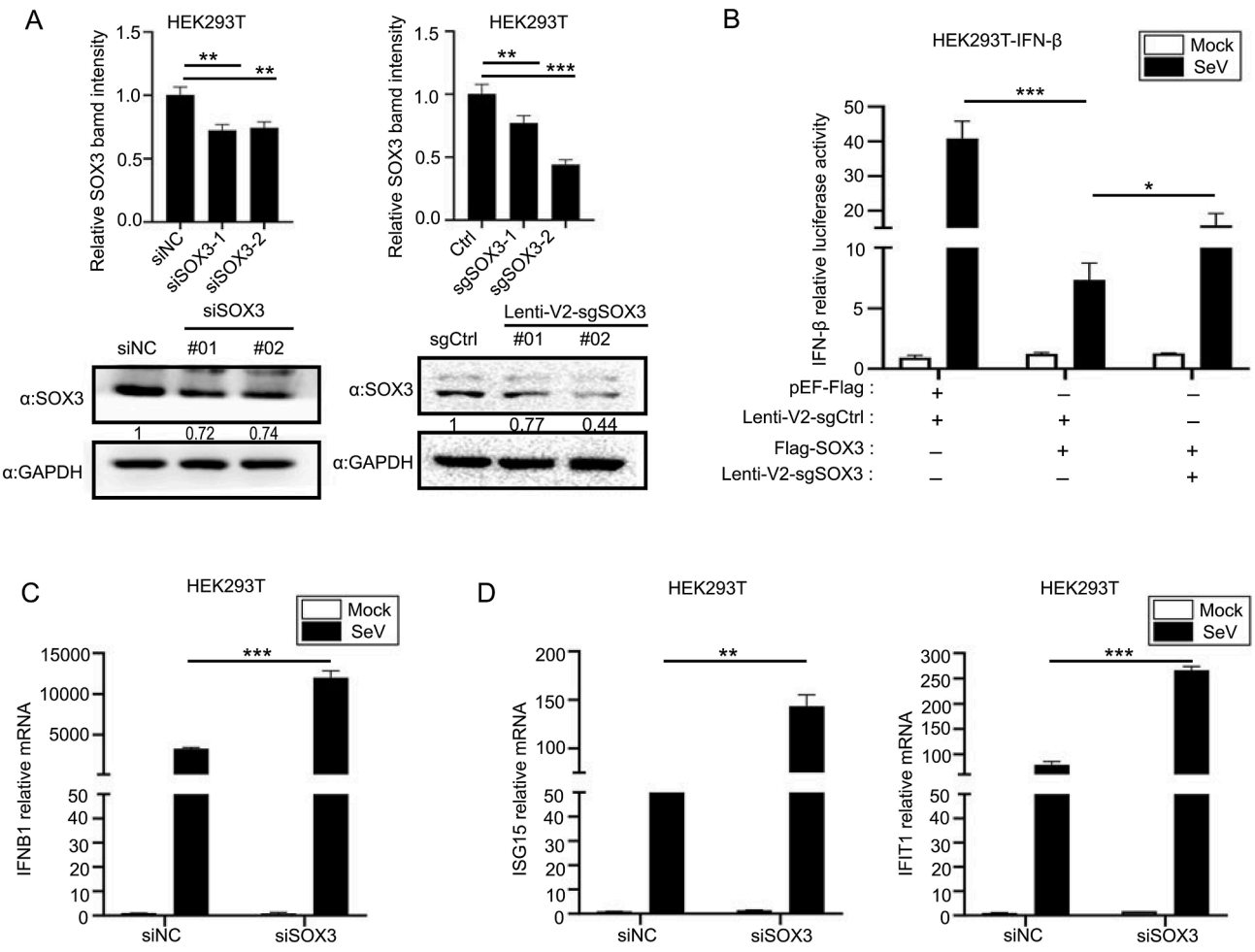

Fig. 4. SOX3 deficiency strengthens antiviral immune signaling. **A** Immunoblot analysis of SOX3 and GAPDH (loading control) in HEK293T cells transfected for 48 h with a non-targeting siNC or siRNA targeting *SOX3* (si*SOX3*-1) (left panel). Immunoblot analysis of SOX3 and GAPDH (loading control) in A549 cells transduced with Lenti-V2-sgCtrl or two independent sgRNAs targeting *SOX3* (Lenti-V2-sg*SOX3* #01 and #02) (right panel). Quantification of SOX3 band intensity normalized to GAPDH (top panel). **B** Luciferase assay analyzing IFNB1 promoter activity in HEK293T cells transfected with IFN-β- firefly luciferase reporter, Renilla luciferase control plasmid, and combinations of Lenti-V2-sgCtrl, Lenti-V2-sgSOX3-1, Lenti-V2-sgSOX3-2, and pEF-Flag-SOX3 as indicated. The experiment used a mixture of both sgSOX3-1 and sgSOX3-2. At 36 h post-transfection, cells were left uninfected (Mock) or infected with SeV (MOI = 10) for 8 h. Data represent relative firefly luciferase activity normalized to Renilla luciferase. **C** Quantitative RT-PCR analysis of *IFNB1* mRNA in HEK293T cells transfected with non-targeting siNC or siRNA targeting *SOX3 (siSOX3-1)*. After 24 h, cells were left stimulated or unstimulated for 8 h with SeV (MOI = 10). **D** Quantitative RT-PCR analysis of *ISG15* (left panel) and *IFIT1* (right panel) mRNA in HEK293T cells transfected with non-targeting siNC or siRNA targeting *SOX3 (siSOX3-1)*. After 24 h, cells were left stimulated or unstimulated for 8 h with SeV (MOI = 10). The *P*-values in (**A**–**D**) were calculated using Student's *t*-test. Data are presented as mean ± SEM, with statistical significance indicated (***$P < 0.001$, **$P < 0.01$, *$P < 0.05$).

infection (Fig. 6B and C). Luciferase reporter assays revealed that SOX3 significantly enhanced the activity of the AKT1 promoter fragments containing peak_387 and peak_389, while mutation of the FIMO-predicted SOX3 binding motifs (CCTCTGTCTG and CTATTGTGAA) abolished this activation (Fig. 6D; Supplementary Fig. S8C; Supplementary Table S5). AKT1 encodes a serine/threonine-protein kinase with crucial roles in cell survival, proliferation, and metabolism and has been implicated in regulating various viral infections (Cohen, 2018; Liu and Cohen, 2015). Given this, we next sought to determine whether SOX3 influences AKT1 expression. To this end, we overexpressed SOX3 in HEK293T and A549 cells and assessed AKT1 expression levels. Immunoblot analysis revealed that SOX3 overexpression led to a dose-dependent increase in AKT1 protein levels, not only upon HSV-1 infection but also upon SeV infection (Fig. 6E).

To validate the interaction between SOX3 and the AKT1 promoter, we performed ChIP assays in HEK293T cells overexpressing Flag-tagged SOX3. Cells were stimulated with SeV to mimic viral infection, and SOX3 occupancy at the AKT1 promoter was subsequently analyzed. Immunoprecipitation with a Flag antibody confirmed successful expression of Flag-SOX3 (Fig. 6F). Importantly, ChIP analysis revealed a significant enrichment of SOX3 binding to the AKT1 promoter region in SeV-stimulated cells compared to unstimulated controls (Fig. 6G). This dynamic regulation of SOX3 binding during viral infection supports the notion that AKT1 may serve as a key downstream effector in SOX3-mediated suppression of antiviral innate immunity.

SOX3 modulates PTEN tail phosphorylation via AKT1 to negatively regulate virus-induced type I interferon expression

Having established AKT1 as a key downstream target of SOX3, we next examined the functional consequences of this interaction in the context of antiviral immune responses. Since SOX3 upregulates AKT1, we investigated whether PTEN, a well-known negative regulator of IFN-I production, acts as a downstream effector in this regulatory axis (Cao et al., 2018; Zhang et al., 2023). Our group previously demonstrated that PTEN dephosphorylates IRF3, promoting its nuclear translocation and subsequent induction of IFN-Is (Li et al., 2016). Moreover, PTEN activity is regulated by phosphorylation at its C-terminal tail, with

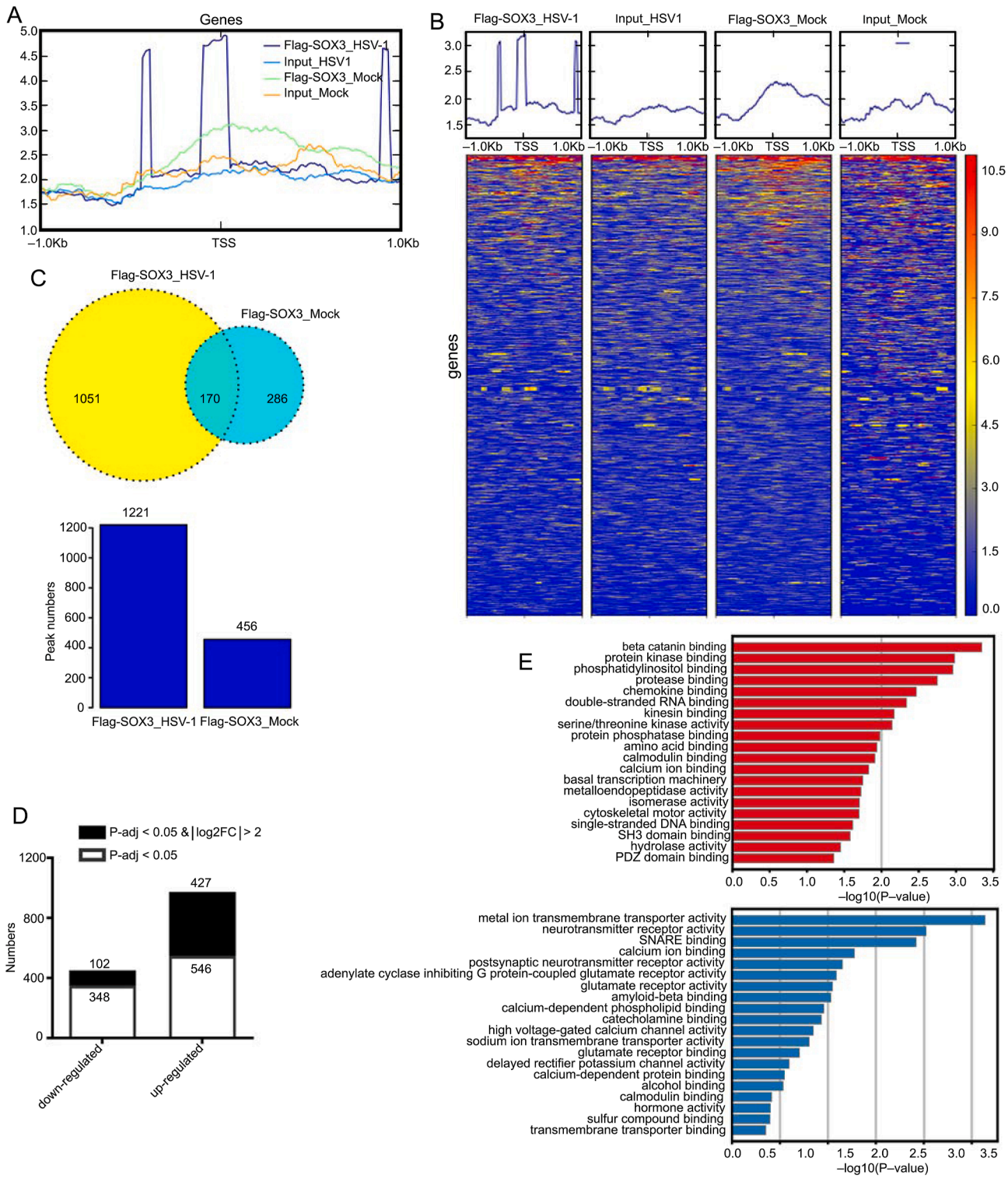

Fig. 5. Atlas of SOX3-HSV-1 binding sites and their potential biological roles based on ChIP-seq data. The cells were transfected for 36 h with plasmids encoding Flag-SOX3 and were then stimulated or left unstimulated with HSV-1 at an MOI of 10 for 12 h. **A** ChIP-seq analysis of SOX3 binding in HEK293T cells with or without HSV-1 infection. Flag-tagged SOX3 was immunoprecipitated using a Flag antibody (Flag-SOX3_HSV-1 and Flag-SOX3_Mock) or IgG (input_HSV-1 and input_Mock). SOX3 binding (average read counts per 50 bp) is plotted relative to the TSS ±1 kb. **B** Signal density plots (top) and heatmaps (bottom) of SOX3 ChIP-seq read distribution around the TSS (±1 kb) in HEK293T cells. Results for Flag-tagged SOX3 immunoprecipitation (Flag-SOX3_HSV-1 and Flag-SOX3_Mock) and IgG controls (input_HSV-1 and input_Mock) are shown. Each heatmap row represents a gene. **C** Venn diagram showing the overlap of SOX3 ChIP-seq peaks (fold change >2, adjusted $P < 0.05$) in HSV-1 infected vs. mock-infected HEK293T cells (top panel). Number of SOX3 ChIP-seq peaks in each condition (bottom panel). **D** Number of upregulated and downregulated differentially expressed genes bound by SOX3 (adjusted $P < 0.05$) in HEK293T cells with vs. without HSV-1 infection. Black bars indicate genes with a fold change ≥2. **E** The bar chart showing pathway enrichment from GO analysis of upregulated (top panel) and downregulated (bottom panel) SOX3-bound genes, with p-values indicated (bottom panel).

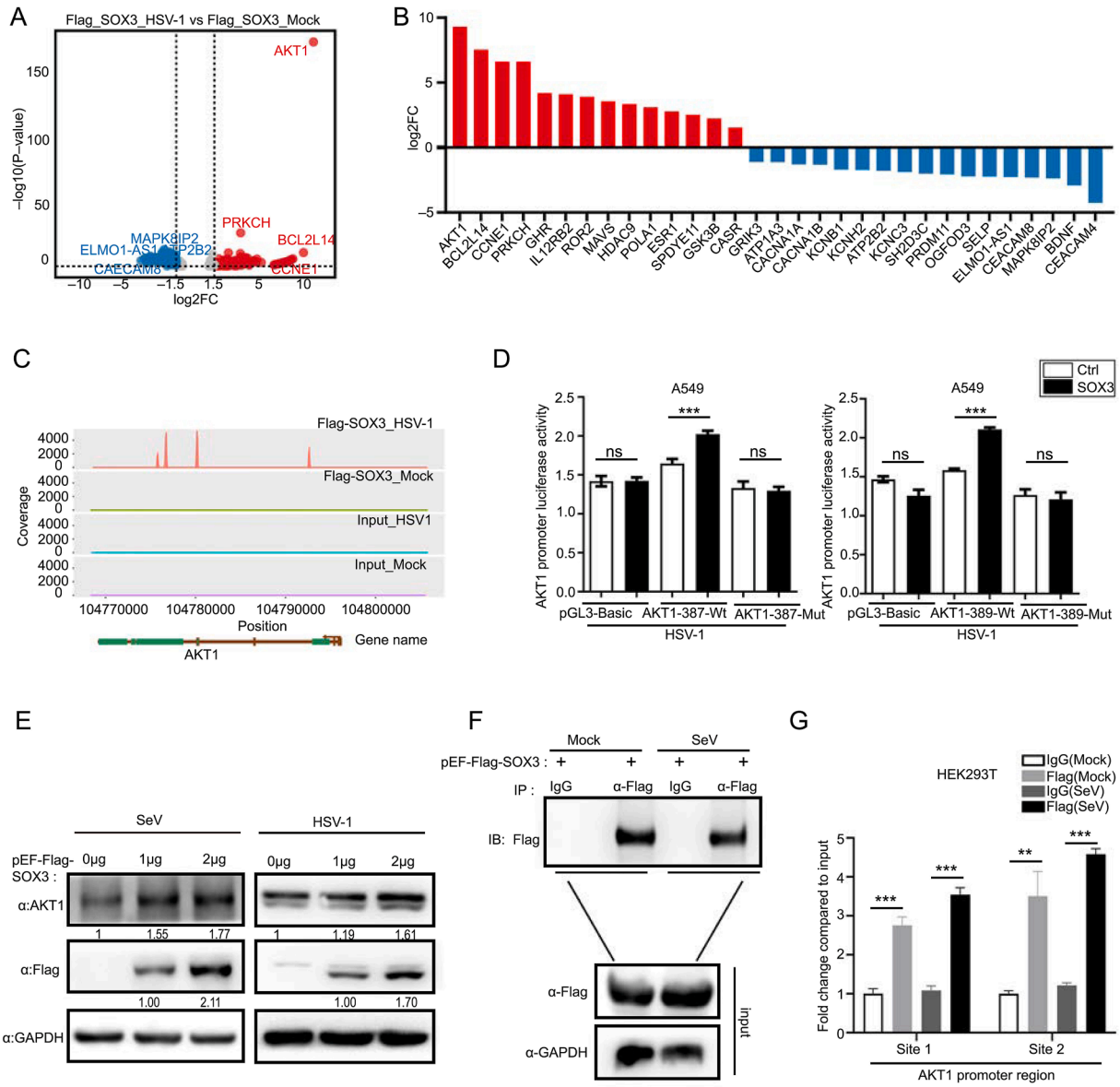

Fig. 6. *AKT1* as a key gene bound by SOX3 revealed through SOX3-HSV-1 ChIP-seq. The cells were transfected for 36 h with plasmids encoding Flag-SOX3 and were then stimulated or left unstimulated with HSV-1 at an MOI of 10 for 12 h. **A** Volcano plot showing differentially expressed genes between Flag-SOX3_HSV-1 and Flag-SOX3_Mock. Upregulated genes are in red, downregulated genes in light blue, with the most significant genes annotated within figure. **B** Bar graph showing SOX3-HSV-1 bound differentially expressed genes, selected based on *P*-adj <0.05 and [log2FC] > 1. **C** ChIP-seq profiles of SOX3 binding at the *AKT1* gene promoter region under Flag-SOX3_HSV-1, input_HSV-1 (MOI = 10, for 12 h infection), Flag-SOX3_Mock, and input_Mock conditions. A schematic of the *AKT1* gene is shown at the bottom of figure. **D** Luciferase reporter assays in A549 cells using pGL3-basic, wild-type (WT), or SOX3-binding site–mutant (Mut) AKT1 promoter constructs revealed that SOX3 significantly enhances transcriptional activity at peak_387 (chr14: 104776499–104776938) and peak_389 (chr14: 104792391–104792641). **E** Immunoblot analysis of AKT1, Flag-SOX3, and GAPDH (loading control) in HEK293T cells transfected with pEF-Flag or increasing doses of pEF-Flag-SOX3 plasmids, and cells were left stimulated with SeV (MOI = 10) for 8 h (left panel) Immunoblot analysis of AKT1, Flag-SOX3, and GAPDH (loading control) in A549 cells transfected with increasing doses (0 μg, 1 μg, 2 μg) of pEF-Flag-SOX3 plasmid. After 36 h, cells were infected with HSV-1 (MOI = 10) for 12 h (right panel). **F-G** Immunoprecipitation and immunoblot (**F**) analysis of Flag-SOX3 and GAPDH (loading control) in HEK293T cells transfected with pEF-Flag-SOX3 plasmids. After 24 h, cells were left stimulated or unstimulated for 8 h with SeV (MOI = 10), followed by chromatin immunoprecipitation (ChIP) analysis of SOX3 occupancy on *AKT1* promoter (**G**). The *P*-values in (**D** and **G**) were calculated using Student's *t*-test. Data are presented as mean ± SEM, with statistical significance indicated (***$P < 0.001$, **$P < 0.01$, *$P < 0.05$).

phosphorylation at Ser380, Thr382, and Thr383 known to inhibit its phosphatase function (Dempsey et al., 2021). Since AKT1is a serine/threonine-protein kinase can phosphorylate PTEN, we hypothesized that SOX3, through its regulation of AKT1, may modulate PTEN activity and consequently influence IFN-I expression.

First, we examined the effect of SOX3 on PTEN phosphorylation. Immunoblot analysis revealed that SOX3 knockdown led to a marked decrease in PTEN phosphorylation in HEK293T cells following SeV stimulation (Fig. 7A). These findings suggest that SOX3 positively regulates PTEN phosphorylation, potentially through its influence on AKT1 activity.

To confirm the role of AKT1 in SOX3-mediated regulation of PTEN, we first validated the efficiency of AKT1 knockdown. Efficient silencing of AKT1 was confirmed by reduced mRNA and protein expression levels (Supplementary Fig. S9A and B). We then assessed PTEN phosphorylation in cells with or without AKT1 knockdown. Immunoblot analysis revealed that AKT1 knockdown abolished the SOX3-induced increase in PTEN phosphorylation, following SeV and HSV-1 stimulation (Fig. 7B;

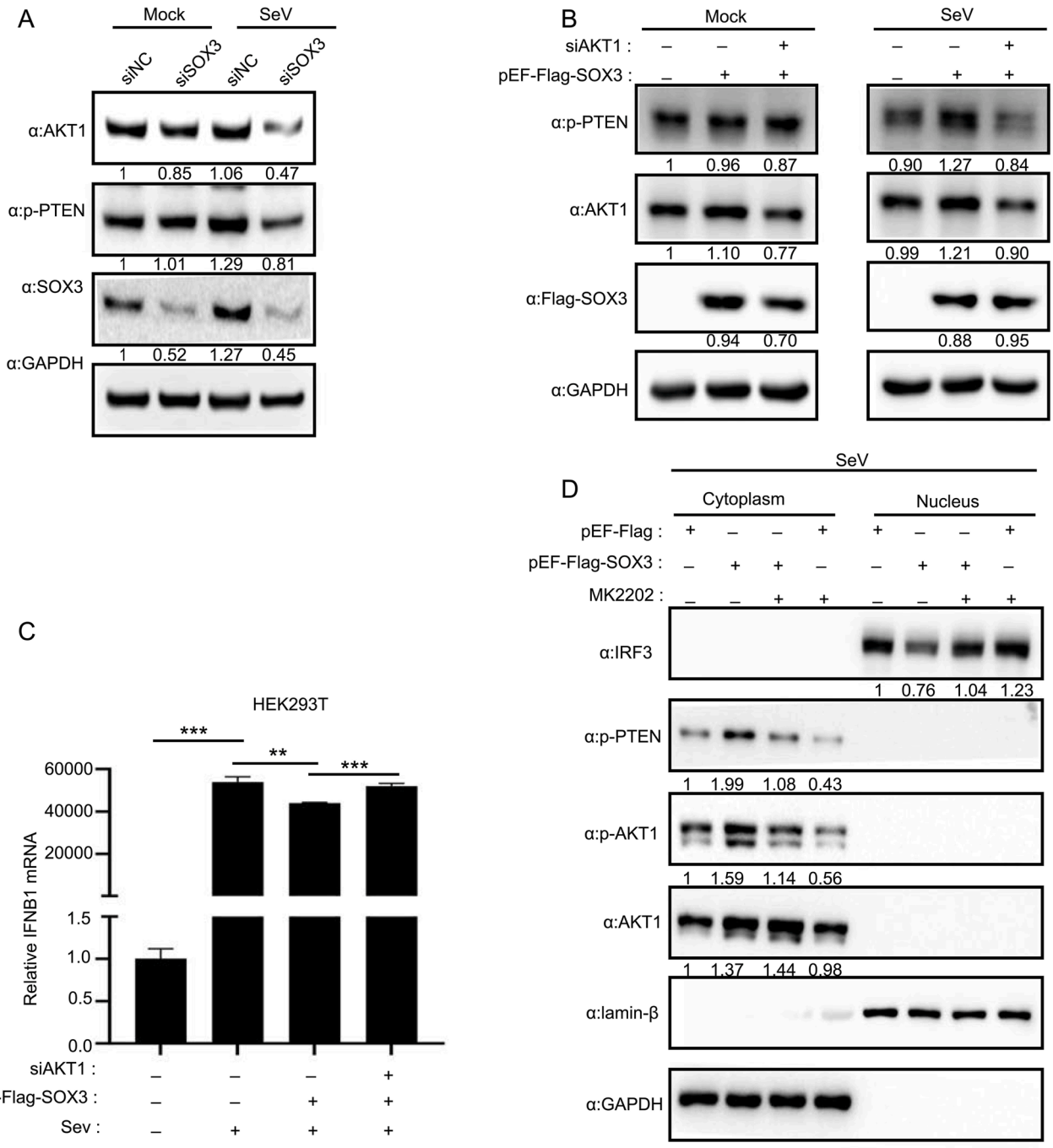

Fig. 7. SOX3-mediated regulation of PTEN tail phosphorylation via AKT1 in virus-induced type I interferon response. **A** Immunoblot analysis of AKT1, p-PTEN, SOX3, and GAPDH (loading control) in HEK293T cells transfected for 24 h with either non-targeting siNC or siRNA targeting *SOX3 (siSOX3-1)*, and cells were left stimulated or unstimulated for 8 h with SeV (MOI = 10). **B** Immunoblot analysis of p-PTEN, AKT1, Flag-SOX3, and GAPDH (loading control) in HEK293T cells transfected for 24 h with non-targeting siNC or siRNA targeting *AKT1 (siAKT1-1)*, along with either pEF-Flag or pEF-Flag-SOX3 plasmids. Cells were either stimulated or unstimulated for 8 h with SeV (MOI = 10). **C** Quantitative RT-PCR analysis of *IFNB1* mRNA in HEK293T cells transfected for 24 h with non-targeting siNC or siRNA targeting *AKT1 (siAKT1-1)*, along with either pEF-Flag or pEF-Flag-SOX3 plasmids. Cells were either stimulated or unstimulated for 8 h with SeV (MOI = 10). The *P*-values were calculated using Student's *t*-test. Data are presented as mean ± SEM, with statistical significance indicated (***$P < 0.001$, **$P < 0.01$, *$P < 0.05$). **D** Immunoblot analysis of cytoplasmic and nuclear fractions from HEK293T cells transfected with pEF-Flag or pEF-Flag-SOX3 plasmids and treated with or without the AKT1 phosphorylation inhibitor MK2206 as indicated. At 24 h post-transfection, cells were infected with SeV (MOI = 10) for 8 h. Blots were probed for IRF3 (to assess nuclear translocation), p-PTEN, p-AKT1, and total AKT1. Lamin-β and GAPDH serve as nuclear and cytoplasmic loading controls, respectively.

Supplementary Fig. S9C). These findings indicate that AKT1 is a key mediator of SOX3-driven PTEN phosphorylation.

Next, we investigated the impact of SOX3 and AKT1 on IFN-I expression. Quantitative RT-PCR analysis revealed that SOX3 overexpression significantly reduced SeV-induced IFNB1 mRNA expression. Notably, this effect was reversed by AKT1 knockdown, indicating that SOX3 and AKT1 exert opposing effects on interferon expression (Fig. 7C). Finally, we evaluated the impact of SOX3 and AKT1 signaling on IRF3 nuclear translocation, a critical step in IFN-I induction. Immunoblot analysis of cytoplasmic and nuclear fractions revealed that SOX3 overexpression markedly reduced SeV- and HSV-1-induced nuclear accumulation of IRF3. Importantly, this suppression was accompanied

by increased phosphorylation of AKT1 and PTEN. Treatment with the AKT1 phosphorylation inhibitor MK2206 restored IRF3 nuclear translocation and concurrently reduced p-AKT1 and p-PTEN levels, despite continued SOX3 overexpression (Fig. 7D; Supplementary Fig. S9D). These findings establish that SOX3 suppresses antiviral responses by enhancing AKT1-dependent PTEN phosphorylation, which impairs IRF3 nuclear translocation and consequently attenuates IFN-I expression.

DISCUSSION

The induction of type I interferon (IFN-I) and inflammatory cytokines is a hallmark of the innate immune response to viral infections (Aoki et al., 2024; Chen et al., 2018). Precise regulation of NF-κB and IFN-I–signaling pathways is essential to ensure effective antiviral response yet avert harmful immunological consequences. Although SOX2 and SOX4 were previously reported to be involved in innate immunity (Shang et al., 2021; Xia et al., 2015), research on SOX3 has predominantly focused on its roles in sex determination and cell differentiation. Given the functional similarities among SOX family proteins, it is plausible that SOX3 is also involved in the innate immune response. Here, we identified a previously unrecognized role for the transcription factor SOX3 in the negative regulation of IFN-I–signaling pathways and host innate immunity.

We initially conducted a comprehensive genome-wide transcriptional analysis that revealed SOX3 overexpression in SeV-infected cells led to the downregulation of several immune response genes, including those involved in IFN-I signaling, antiviral defense, and proinflammatory cytokines. Next, we confirmed that SOX3 overexpression potently suppressed IFN-β promoter activation and mRNA expression in a dose-dependent manner. This effect was observed in both the early and late phases of IFN production, suggesting that SOX3 broadly targets the IFN pathway. Interestingly, we observed that SOX3 expression is induced by SeV, VSV, or HSV-1 infection at both the mRNA and protein levels in THP-1 cells. This suggests a potential mechanism by which viruses can exploit host factors to their advantage. Indeed, several viruses have evolved strategies to manipulate host protein expression to facilitate their replication and spread (García-Sastre, 2017; Walsh and Mohr, 2011).

Although SOX3 overexpression produced modest basal increases in selected interferon/ISG transcripts (e.g., IFNE, IFIT3, IFIH1, IFI6), these likely reflect compensatory responses to SOX3 overexpression rather than a pro-antiviral function; upon viral stimulation, SOX3 consistently attenuated antiviral signaling, reducing IFNB1 and downstream ISG induction, supporting a context-dependent negative-regulatory role during infection (Fig. 8). Furthermore, SOX3 overexpression inhibited the activation of key signaling molecules upstream of IFN-β, including RIG-I, TBK1, and MAVS. These results indicate that SOX3 interferes with the sensing of viral infection and the initiation of antiviral signaling cascades. This is consistent with previous studies demonstrating that viral proteins can antagonize PRR signaling pathways to evade host detection (Bowie and Unterholzner, 2008; Chan and Gack, 2016). Importantly, SOX3 also suppressed the activation of ISRE and NF-κB, transcription factors that drive the expression of ISGs and inflammatory mediators. This suggests that SOX3 not only inhibits the initial production of IFN-β but also dampens the downstream effects of IFN signalling, further compromising the host's ability to mount an effective antiviral response. The ability of SOX3 to modulate both ISRE and NF-κB signaling suggests a broader role in regulating immune responses, as NF-κB is a central regulator of inflammation and is implicated in various immune processes (Capece et al., 2022; Liu et al., 2017).

While our mechanistic investigation focused on the SOX3-AKT1-PTEN axis, the innate immune response is inherently complex and likely involves extensive crosstalk with additional pathways such as NF-κB and STAT signaling. Future studies integrating RNA-seq with SOX3 ChIP-seq will be instrumental in identifying additional SOX3-regulated targets (e.g., SOCS1, SOCS3) and determining whether SOX3 directly modulates these loci to influence NF-κB/STAT activation and IFN-I output. Such systems-level analyses will help delineate how SOX3 orchestrates broader regulatory networks beyond the AKT1-PTEN pathway to fine-tune antiviral immunity.

Conversely, the knockdown of SOX3 enhanced IFN-β production and ISG expression, further supporting its role as a negative regulator of antiviral immunity. These findings are consistent with the observation that SOX3 expression is induced by viral infection, reinforcing the concept that viruses can exploit SOX3 to evade host defenses. This highlights the complex interplay between viruses and host factors, where viruses can manipulate host proteins to their advantage. Several viruses have evolved strategies to interfere with IFN production or signaling, allowing them to establish persistent infections.

To elucidate the mechanism underlying SOX3-mediated suppression of IFN responses, we performed ChIP-seq analysis and identified AKT1 as a key target gene directly bound and upregulated by SOX3. AKT1 is a serine/threonine kinase with diverse roles in cell survival, proliferation, and metabolism. Our findings demonstrate that SOX3-mediated

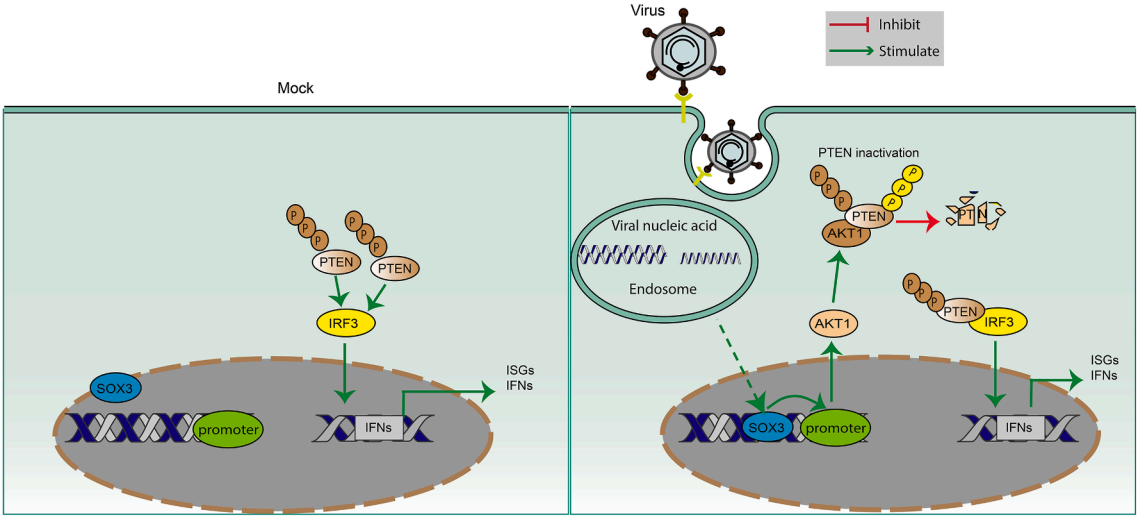

Fig. 8. SOX3 regulates antiviral immunity via the AKT1-PTEN pathway. In the mock condition (left), SOX3 fails to activate AKT1, keeping PTEN active. Upon viral infection (right), SOX3 activates AKT1, inactivates PTEN, and disrupts IRF3 translocation, resulting in reduced IFN-β and ISG expression.

upregulation of AKT1 leads to increased phosphorylation and, as a result, inactivation of PTEN, which is a known modulator of IRF3 activity. PTEN has been shown to dephosphorylate IRF3, promoting its nuclear translocation and activation of IFN-I expression. Therefore, by inhibiting PTEN activity, SOX3 impairs IRF3 nuclear translocation and diminishes IFN-I production. The AKT-PTEN axis plays a central role in regulating various cellular processes (Kamo et al., 2013; Tsai et al., 2024; Vidotto et al., 2020). This finding provides new insights into the AKT-PTEN axis, highlighting its essential role in regulating antiviral immune responses. Our findings demonstrate that SOX3 suppresses virus-induced IFN-β activation and signaling, highlighting its potential role in immune evasion and viral pathogenesis by directly modulating signaling molecules, including AKT1 and PTEN.

CONCLUSION

In conclusion, this study uncovers a previously unrecognized role of SOX3 in regulating IFN-I responses and highlights its significance in antiviral immunity. Our findings identify SOX3 as a potential therapeutic target for modulating interferon signaling during viral infection. Future studies should further investigate the SOX3-AKT1-PTEN axis across diverse viral models, assess its relevance in other cell types and *in vivo* systems, and explore strategies to therapeutically target SOX3 to enhance antiviral defense.

MATERIALS AND METHODS

Plasmids, ligands, sgRNAs, and siRNAs

The eukaryotic expression vector pEF-Flag was obtained from Professor Zhi-Jian Chen's laboratory (Southwestern Medical Research Center, USA). RIG-I, TBK1, and MAVS expression constructs were previously generated in our laboratory. The *SOX3* gene fragment was amplified from HEK293T cell cDNA and cloned into the pEF-Flag vector using *Xho*I/*Mlu*I restriction sites. The *AKT1* gene fragment was similarly cloned into pEF-Flag. The pGL3-IFN-β promoter luciferase reporter plasmid was obtained from Professor Hong-Bing Shu's laboratory (Wuhan University Medical School). Dual-luciferase reporter system plasmids (pGL3-basic and pRL-TK-Renilla) were purchased from Promega (USA). AKT1-Promoter clones (chr14: 104792360–104792657 and 104776286–104777753) were cloned into pGL3-basic using *Xho*I and *Mlu*I restriction enzymes. Bacterial lipopolysaccharide (LPS) and poly (I:C) were purchased from Sigma (USA). siRNAs targeting SOX3 (si*SOX3*), AKT1 (si*AKT1*), and a non-targeting siNC were purchased from Guangzhou RiboBio Co., Ltd. All constructs were verified by DNA sequencing. siRNA, sgRNA sequences, and primers used for construct generation are listed in Supplementary Table S6.

Cell culture, transfection, and viral stimulation

HEK293T, RAW264.7, A549, and THP-1 cell lines were used in this study. HEK293T cells were obtained from the China Center for Type Culture Collection. THP-1, A549, and RAW264.7 cells were provided by Professor Ming-Xiong Guo's laboratory (School of Life Sciences, Wuhan University). All cells were cultured in DMEM (Gibco/Life Technologies, Thermo Fisher Scientific, Waltham, MA, USA) supplemented with 10% FBS (Gibco/Life Technologies) and 1% penicillin-streptomycin solution at 37 °C in a humidified 5% CO_2 incubator.

For transfection experiments, cells were transfected with plasmids (200 ng–1000 ng) or siRNAs (50–100 nM) using Lipofectamine 2000 (Invitrogen, Thermo Fisher Scientific) according to the manufacturer's instructions. After 24 or 36 h, cells were stimulated with SeV, VSV, HSV-1, or specific ligands for 8–12 h. SeV, VSV, and HSV-1 were sourced from our laboratory.

Luciferase reporter assays

HEK293T, A549, and RAW264.7 cells were seeded on 24-well plates and incubated for 12 h prior to transfection. Cells were co-transfected with the firefly luciferase reporter constructs (IFN-β, ISRE, NF-κB), pRL-TK-Renilla, and increasing doses of pEF-Flag-SOX3. pEF-Flag, pEF-RIG-I, TBK1, and MAVS were also included as indicated. Luciferase activity was measured using the Dual-Luciferase Reporter Assay System (Promega) according to the manufacturer's instructions. Firefly luciferase activity was normalized to Renilla luciferase activity to control for transfection efficiency.

RNA extraction and quantitative real-time PCR (qPCR)

Total RNA was isolated using TRIzol reagent (Invitrogen). cDNA was synthesized using the PrimeScript RT Reagent Kit (Takara, Japan). qPCR was performed using the SYBR PrimeScript RT-PCR Kit (Takara). GAPDH served as an internal control. Relative gene expression levels were determined using the $2^{-\Delta\Delta Ct}$ method, where *Ct* represents the PCR cycle threshold. All the qPCR primers are listed in Supplementary Table S7.

Western blotting

Cells were lysed using RIPA lysis and protein extraction buffer (Beyotime, Shanghai, China). Protein concentrations were determined using the enhanced BCA protein assay kit (Beyotime). Equal amounts of protein were separated by SDS-PAGE and transferred to nitrocellulose membranes (Millipore, Billerica, MA). Membranes were blocked with 5% non-fat dry milk in Tris-buffered saline with Tween-20 [TBS-T; 120 mM Tris-HCl (pH 7.4), 150 mM NaCl, 0.1% Tween 20] and incubated with primary antibodies followed by appropriate secondary antibodies.

The following antibodies were used: SOX3 (Santa Cruz, cat. no. sc-20089), AKT1 (Cell Signaling Technology, cat. no. 75692), Phospho-AKT1 (Cell Signaling Technology, cat. no. 4060S), Phospho-PTEN (Cell Signaling Technology, cat. no. 9188S), Flag (Proteintech, cat. no. 20543-1-AP), GAPDH (Proteintech, cat. no. 10494-1-AP), and α-Tubulin (ABclonal, cat. no. A12289).

Nuclear and cytoplasmic protein fractionation

Nuclear and cytoplasmic protein fractions were isolated using the Nuclear and Cytoplasmic Protein Extraction Kit (Prellygen Gene Technology Co., Ltd., Cat. No. P1200) according to the manufacturer's protocol. Protease inhibitors were included throughout. Fraction purity was confirmed by Western blotting using GAPDH or α-Tubulin (cytoplasmic markers) and lamin-β (nuclear marker). The resulting fractions were subsequently used for Western blot analysis.

Chromatin immunoprecipitation (ChIP) assay

ChIP assays were performed using HEK293T cells transfected with SOX3. Briefly, cells were fixed with 1% formaldehyde and lysed. Chromatin was sheared using an ultrasonic cell disruptor. Protein-DNA complexes were immunoprecipitated with normal IgG or anti-FLAG M2 agarose beads (Sigma-Aldrich). Following immunoprecipitation, cross-links were reversed, and DNA was purified. Specific primers were used to amplify the AKT1 promoter region from the immunoprecipitated DNA.

RNA sequencing analysis

RNA sequencing (RNA-Seq) was conducted to analyze gene expression profiles across four experimental conditions: SOX3, SOX3SeV, VEC, and VECSeV. Total RNA was extracted, and libraries were prepared

using the Illumina platform for paired-end sequencing (6 GB per sample) with the UID-mRNA-seq PE-150 method. Raw data were pre-processed with FastQC for quality assessment and trimmed using Trimmomatic to remove low-quality reads. Clean reads were aligned to the Homo sapiens GRCh38 reference genome using HISAT2, and gene expression levels were quantified in RPKM (Reads Per Kilobase per Million Reads) to normalize for gene length and sequencing depth. Differentially expressed genes (DEGs) were identified using edgeR with a logFC >1 and *P*-value <0.05. GO and KEGG pathway enrichment analyses were performed using the online METASCAPE tool. Biological replicate correlation was evaluated with Spearman correlation, and sample similarity was further assessed using hierarchical clustering and PCA. Volcano plots were generated for DEG visualization. All analyses were conducted using standard bioinformatics pipelines, with statistical significance set at $P < 0.05$, and results were visualized in R (version 4.2.2).

ChIP-sequencing (ChIP-seq) and data analysis

ChIP-sequencing (ChIP-seq) analysis was conducted across two experimental conditions: Flag_SOX3_HSV-1 and Flag_SOX3_Mock. ChIP-seq libraries were prepared using DNA isolated from ChIP assays, using standard protocols. DNA was purified using a commercial kit (e.g., Qiagen) and sheared to approximately 200–400 bp fragments. Sequencing was performed on an Illumina HiSeq 2500 platform with paired-end 150 bp reads. Raw sequence data (FASTQ format) were quality-checked using FastQC and trimmed using Trim Galore. Trimmed reads were aligned to the human genome (GRCh38) using the Burrows-Wheeler Aligner (BWA). Alignment quality was assessed with SAMtools. Duplicate reads were removed using Picard tools. Peak calling was performed using MACS2 (version 2.1.1) with *P*-values < 1e-5 and q-values <0.05. Differential binding analysis was conducted using DESeq2. Gene Ontology (GO) enrichment analysis was performed using the online METASCAPE tool.

Statistical analysis

Statistical analyses and graphs were generated using GraphPad Prism 6.0 (GraphPad Software Inc., San Diego, CA, USA). Data are presented as mean ± standard deviation (SD) unless otherwise noted. A two-tailed Student's *t*-test was used for comparisons between groups. A *P*-value <0.05 was considered statistically significant. All experiments were performed with a minimum of three biological replicates. "ns" denotes no significant difference. $*P < 0.05$, $**P < 0.01$, and $***P < 0.001$ indicate different levels of significance.

DATA AVAILABILITY

All the data generated during the current study are included in the manuscript.

ETHICS STATEMENT

This article does not contain any studies with human or animal subjects performed by any of the authors.

AUTHOR CONTRIBUTIONS

Tanzeel Yousaf: conceptualization, investigation, methodology, data curation, writing-original draft, software; Jianwen Chen: conceptualization & investigation; Wajeeha Naz: investigation, data curation, writing review & editing; Jiaqi Xu; investigation; Ying Liu: validation; Junsong Huang: validation; Siqi Yang: validation; Jing Zhang: validation; Iram Amin: validation; Mingxiong Guo; resources & supervision; Yunlan Tang: conceptualization, data curation, funding & acquisition; Guihong Sun: conceptualization, methodology, investigation, data curation, funding acquisition, project administration, resources & writing review.

CONFLICT OF INTEREST

The authors have declared that no competing interest exists.

ACKNOWLEDGEMENT

This work was supported by the Central Guidance on Local Science and Technology Development Fund of Tibet (Grant No. XZ202301YD0040C), the National Natural Science Foundation of China (Grant No. 32260173), and the Youth Program of Natural Science Foundation of Henan Province (Grant No. 252300420594).

APPENDIX A. SUPPLEMENTARY DATA

Supplementary data to this article can be found online at https://doi.org/10.1016/j.virs.2025.11.012.

REFERENCES

Aoki, A., Iwamura, C., Kiuchi, M., Tsuji, K., Sasaki, A., Hishiya, T., Hirasawa, R., Kokubo, K., Kuriyama, S., Onodera, A., Shimada, T., Nagaoka, T., Ishikawa, S., Kojima, A., Mito, H., Hase, R., Kasahara, Y., Kuriyama, N., Nakamura, S., Urushibara, T., Kaneda, S., Sakao, S., Nishida, O., Takahashi, K., Kimura, M.Y., Motohashi, S., Igari, H., Ikehara, Y., Nakajima, H., Suzuki, T., Hanaoka, H., Nakada, T., Kikuchi, T., Nakayama, T., Yokote, K., Hirahara, K., 2024. Suppression of type I interferon signaling in myeloid cells by autoantibodies in severe COVID-19 patients. J. Clin. Immunol. 44, 104.

Bowie, A.G., Unterholzner, L., 2008. Viral evasion and subversion of pattern-recognition receptor signalling. Nat. Rev. Immunol. 8, 911–922.

Cao, Y., Wang, H., Yang, L., Zhang, Z., Li, C., Yuan, X., Bu, L., Chen, L., Chen, Y., Li, C.-M., Guo, D., 2018. PTEN-L promotes type I interferon responses and antiviral immunity. Cell. Mol. Immunol. 15, 48–57.

Capece, D., Verzella, D., Flati, I., Arboretto, P., Cornice, J., Franzoso, G., 2022. NF-κB: blending metabolism, immunity, and inflammation. Trends Immunol. 43, 757–775.

Chan, Y.K., Gack, M.U., 2016. Viral evasion of intracellular DNA and RNA sensing. Nat. Rev. Microbiol. 14, 360–373.

Chen, S., Bonifati, S., Qin, Z., St Gelais, C., Kodigepalli, K.M., Barrett, B.S., Kim, S.H., Antonucci, J.M., Ladner, K.J., Buzovetsky, O., Knecht, K.M., Xiong, Y., Yount, J.S., Guttridge, D.C., Santiago, M.L., Wu, L., 2018. SAMHD1 suppresses innate immune responses to viral infections and inflammatory stimuli by inhibiting the NF-κB and interferon pathways. Proc. Natl. Acad. Sci. U.S.A 115, E3798–E3807.

Cohen, J.I., 2018. Herpesviruses in the activated Phosphatidylinositol-3-Kinase-δ syndrome. Front. Immunol. 9, 237.

de Jesus, J.R., de Araújo Andrade, T., 2020. Understanding the relationship between viral infections and trace elements from a metallomics perspective: implications for COVID-19. Metallomics 12, 1912–1930.

Del Puerto, H.L., Miranda, A.P.G.S., Qutob, D., Ferreira, E., Silva, F.H.S., Lima, B.M., Carvalho, B.A., Roque-Souza, B., Gutseit, E., Castro, D.C., Pozzolini, E.T., Duarte, N. O., Lopes, T.B.G., Taborda, D.Y.O., Quirino, S.M., Elgerbi, A., Choy, J.S., Underwood, A., 2024. Clinical correlation of transcription factor SOX3 in cancer: unveiling its role in tumorigenesis. Genes 15, 777.

Dempsey, D.R., Viennet, T., Park, E., Henriquez, S., Chen, Z., Jeliazkov, J.R., Phan, K.L., Coote, P., Gray, J.J., Eck, M.J., Gabelli, S.B., Arthanari, H., Cole, P.A., 2021. The structural basis of PTEN regulation by multi-site phosphorylation. Nat. Struct. Mol. Biol. 28, 858–868.

Diamond, M.S., Farzan, M., 2013. The broad-spectrum antiviral functions of IFIT and IFITM proteins. Nat. Rev. Immunol. 13, 46–57.

Fensterl, V., Sen, G.C., 2009. Interferons and viral infections. BioFactors Oxf. Engl. 35, 14–20.

García-Sastre, A., 2017. Ten strategies of interferon evasion by viruses. Cell Host Microbe 22, 176–184.

Hendy, G.N., Canaff, L., 2016. Calcium-sensing receptor, proinflammatory cytokines and calcium homeostasis. Semin. Cell Dev. Biol. 49, 37–43.

Hsu, M.-J., Wu, C.-Y., Chiang, H.-H., Lai, Y.-L., Hung, S.-L., 2010. PI3K/Akt signaling mediated apoptosis blockage and viral gene expression in oral epithelial cells during herpes simplex virus infection. Virus Res. 153, 36–43.

Jang, J.-H., Shin, H.W., Lee, J.M., Lee, H.-W., Kim, E.-C., Park, S.H., 2015. An overview of pathogen recognition receptors for innate immunity in dental pulp. Mediat. Inflamm. 2015, 794143.

Jiang, J., Wang, Yufei, Sun, M., Luo, X., Zhang, Z., Wang, Yijun, Li, S., Hu, D., Zhang, J., Wu, Z., Chen, X., Zhang, B., Xu, X., Wang, S., Xu, S., Huang, W., Xia, L., 2024. SOX on tumors, a comfort or a constraint? Cell Death Discov. 10, 1–18.

Kamo, N., Ke, B., Busuttil, R.W., Kupiec-Weglinski, J.W., 2013. PTEN-MEDIATEDAKT/β-CATENIN/FOXO1 signaling regulates innate immune responses in mouse liver ischemia/reperfusion injury. Hepatol. Baltim. Md 57, 289–298.

Kasuga, Y., Zhu, B., Jang, K.-J., Yoo, J.-S., 2021. Innate immune sensing of coronavirus and viral evasion strategies. Exp. Mol. Med. 53, 723–736.
Kishimoto, K., Wilder, C.L., Buchanan, J., Nguyen, M., Okeke, C., Hoffmann, A., Cheng, Q.J., 2021. High dose IFN-β activates GAF to enhance expression of ISGF3 target genes in MLE12 epithelial cells. Front. Immunol. 12, 651254.
Lang, R., Li, H., Luo, X., Liu, C., Zhang, Y., Guo, S., Xu, J., Bao, C., Dong, W., Yu, Y., 2022. Expression and mechanisms of interferon-stimulated genes in viral infection of the central nervous system (CNS) and neurological diseases. Front. Immunol. 13, 1008072.
Lee, Y.-R., Chen, M., Pandolfi, P.P., 2018. The functions and regulation of the PTEN tumour suppressor: new modes and prospects. Nat. Rev. Mol. Cell Biol. 19, 547–562.
Li, S., Zhu, M., Pan, R., Fang, T., Cao, Y.-Y., Chen, S., Zhao, X., Lei, C.-Q., Guo, L., Chen, Y., Li, C.-M., Jokitalo, E., Yin, Y., Shu, H.-B., Guo, D., 2016. The tumor suppressor PTEN has a critical role in antiviral innate immunity. Nat. Immunol. 17, 241–249.
Liu, T., Zhang, L., Joo, D., Sun, S.-C., 2017. NF-κB signaling in inflammation. Signal Transduct. Targeted Ther. 2, 1–9.
Liu, X., Cohen, J.I., 2015. The role of PI3K/Akt in human herpesvirus infection: from the bench to the bedside. Virology 479–480, 568–577.
Liu, Y., Song, F., Zeng, X., Yang, S., Zhai, Z., Wang, Z., Naz, W., Yousaf, T., Sun, J., Zhang, Y., Zhou, Y., Guo, M., Shi, Y.-B., Tian, G., Sun, G., 2025. The AKT1-mTOR signaling cascade is crucial for SOX3 to promote hepatocarcinogenesis. Genes Dis. 12, 101316.
McDougal, M.B., Maria, A.M.D., Nakahara, E., Boys, I.N., Schoggins, J.W., 2024. IFIT1 is rapidly evolving and exhibits disparate antiviral activities across 11 mammalian orders. eLife 13. RP101929.
Ning, S., Pagano, J.S., Barber, G.N., 2011. IRF7: activation, regulation, modification and function. Gene Immun. 12, 399–414.
Perng, Y.-C., Lenschow, D.J., 2018. ISG15 in antiviral immunity and beyond. Nat. Rev. Microbiol. 16, 423–439.
Popli, S., Chakravarty, S., Fan, S., Glanz, A., Aras, S., Nagy, L.E., Sen, G.C., Chakravarti, R., Chattopadhyay, S., 2022. IRF3 inhibits nuclear translocation of NF-κB to prevent viral inflammation. Proc. Natl. Acad. Sci. U.S.A 119, e2121385119.
Schneider, W.M., Chevillotte, M.D., Rice, C.M., 2014. Interferon-stimulated genes: a complex web of host defenses. Annu. Rev. Immunol. 32, 513–545.
Shang, J., Zheng, Y., Mo, J., Wang, W., Luo, Z., Li, Y., Chen, X., Zhang, Q., Wu, K., Liu, W., Wu, J., 2021. Sox4 represses host innate immunity to facilitate pathogen infection by hijacking the TLR signaling networks. Virulence 12, 704–722.
Steinbach, N., Hasson, D., Mathur, D., Stratikopoulos, E.E., Sachidanandam, R., Bernstein, E., Parsons, R.E., 2019. PTEN interacts with the transcription machinery on chromatin and regulates RNA polymerase II-mediated transcription. Nucleic Acids Res. 47, 5573–5586.
Stow, J.L., Manderson, A.P., Murray, R.Z., 2006. SNAREing immunity: the role of SNAREs in the immune system. Nat. Rev. Immunol. 6, 919–929.
Sun, L., Wang, X., Saredy, J., Yuan, Z., Yang, X., Wang, H., 2020. Innate-adaptive immunity interplay and redox regulation in immune response. Redox Biol. 37, 101759.
Takeuchi, O., Akira, S., 2009. Innate immunity to virus infection. Immunol. Rev. 227, 75–86.
Tavares, L.P., Negreiros-Lima, G.L., Lima, K.M., E Silva, P.M.R., Pinho, V., Teixeira, M. M., Sousa, L.P., 2020. Blame the signaling: role of cAMP for the resolution of inflammation. Pharmacol. Res. 159, 105030.
Taylor, H., Laurence, A.D.J., Uhlig, H.H., 2019. The role of PTEN in innate and adaptive immunity. Cold Spring Harb. Perspect. Med. 9, a036996.
Tsai, P.-J., Chen, M.-Y., Hsu, W.-C., Lin, S.-F., Chan, P.-C., Chen, H.-H., Kao, C.-Y., Lin, W.-J., Chuang, T.-H., Yu, G.-Y., Su, Y.-W., 2024. PTEN acts as a crucial inflammatory checkpoint controlling TLR9/IL-6 axis in B cells. iScience 27, 110388.
Vidotto, T., Melo, C.M., Castelli, E., Koti, M., Dos Reis, R.B., Squire, J.A., 2020. Emerging role of PTEN loss in evasion of the immune response to tumours. Br. J. Cancer 122, 1732–1743.
Vig, M., Kinet, J.-P., 2009. Calcium signaling in immune cells. Nat. Immunol. 10, 21.
Walsh, D., Mohr, I., 2011. Viral subversion of the host protein synthesis machinery. Nat. Rev. Microbiol. 9, 860–875.
Wan, X., Zhou, M., Huang, F., Zhao, N., Chen, Xu, Wu, Y., Zhu, W., Ni, Z., Jin, F., Wang, Y., Hu, Z., Chen, Xianguo, Ren, M., Zhang, H., Zha, X., 2021. AKT1-CREB stimulation of PDGFRα expression is pivotal for PTEN deficient tumor development. Cell Death Dis. 12, 172.
Xia, P., Wang, S., Ye, B., Du, Y., Huang, G., Zhu, P., Fan, Z., 2015. Sox2 functions as a sequence-specific DNA sensor in neutrophils to initiate innate immunity against microbial infection. Nat. Immunol. 16, 366–375.
Yang, X., Zhao, S., Yuan, H., Shi, R., Gu, W., Gu, Z., Lu, X., Zhao, H., 2020. Knockdown of Ror2 suppresses TNF-α-induced inflammation and apoptosis in vascular endothelial cells. Mol. Med. Rep. 22, 2981–2989.
Zhang, J., Zhang, Y., Lin, X., Han, X., Meredith, K.L., Li, Z., 2023. The effects of the tumor suppressor gene PTEN on the proliferation and apoptosis of breast cancer cells via AKT phosphorylation. Transl. Cancer Res. 12, 1863–1872.
Zhang, M., Li, J., Yan, H., Huang, J., Wang, F., Liu, T., Zeng, L., Zhou, F., 2021. ISGylation in innate antiviral immunity and pathogen defense responses: a review. Front. Cell Dev. Biol. 9, 788410.
Zhang, Y., Wang, X., Yang, H., Liu, H., Lu, Y., Han, L., Liu, G., 2013. Kinase AKT controls innate immune cell development and function. Immunology 140, 143–152.